

Synthesis and spectroscopic properties of (N/O) mono- and dispirocyclotriphosphazene derivatives with benzyl pendant arms: study of biological activity*

Özlem İŞCAN¹ , Reşit CEMALOĞLU¹ , Nuran ASMAFİLİZ^{1,**} , Zeynel KILIÇ¹ ,
Leyla AÇIK² , Pelin ÖZBEDEN² , Tuncer HÖKELEK³ 

¹Department of Chemistry, Faculty of Science, Ankara University, Ankara, Turkey

²Department of Biology, Faculty of Science, Gazi University, Ankara, Turkey

³Department of Physics, Faculty of Science, Hacettepe University, Beytepe, Ankara, Turkey

Received: 07.08.2019

Accepted/Published Online: 12.10.2019

Final Version: 11.02.2020

Abstract: The Cl replacement reactions of hexachlorocyclotriphosphazene (trimer; $N_3P_3Cl_6$) with sodium (N-benzyl)-aminopropanoxides (**1** and **2**) produced monospiro- (**3** and **4**), cis-, and trans-dispirocyclotriphosphazenes (**13–16**). The monospiro tetrakis-aminocyclotriphosphazenes (**5–12**) were obtained by the Cl substitutions of **3** and **4** with different secondary amines. The cis- (**13** and **14**) and trans-dispirophosphazenes (**15** and **16**) possessed 2 chiral P centers, and they were able to present meso and racemic forms, respectively. Moreover, the structures of compounds **5** and **14** were designated using X-ray data. The absolute configuration of compound **14** was found as SR in the solid state. Analytical and spectroscopic data of the phosphazenes were consistent with their suggested structures. Antimicrobial activities of the benzyl-pendant-armed cyclotriphosphazenes were scrutinized against G(+) and G(–) bacteria and yeast strains. The bacterium most affected by the synthesized compounds was *Pseudomonas aeruginosa*. Minimum inhibitory concentrations and minimal bacterial concentrations were in the range of 125–500 μ M. Interactions between the phosphazenes (**3–12** and **15**) and plasmid DNA were studied with agarose gel electrophoresis. The phosphazene-DNA interaction studies of the cyclotriphosphazenes revealed that phosphazenes **3**, **4**, and **15** had a substantial effect on supercoiled DNA by cleavage of the double helix.

Key words: Pendant-armed spirocyclotriphosphazenes, crystal structure, spectroscopy, antimicrobial activity, DNA interaction

1. Introduction

Phosphazenes refer to phosphorus-nitrogen compounds that occur by the sequential bonding of atoms to each other [1,2]. Hexachlorocyclotriphosphazene ($N_3P_3Cl_6$, trimer) is versatile and has the ability to react easily with different mono-, di-, and multifunctional reagents [3–5]. When trimer is reacted with monofunctional agents, at least 6 different cyclotriphosphazene derivatives can be formed [6]. In addition, the Cl replacement reactions of trimer with one equimolar difunctional reagent may predominantly yield monospiro products when compared to other expected ansa- and bino-isomers [7,8]. Moreover, when two equimolar difunctional agents are used, dispirocyclotriphosphazenes with cis- and trans-geometrical and meso/racemic optical isomers can occur [9–11]. It is difficult to separate these isomers from each other; hence, very few optical and

*This manuscript is dedicated to Prof. Dr. Adem Kılıç on his retirement.

**Correspondence: gurun@science.ankara.edu.tr

geometrical isomers of dispiro derivatives have been separated in the literature [9–13]. Geometric isomers of dispirocyclotriphosphazenes can be separated by column chromatography, while optical isomers may be determined using ^{31}P $\{^1\text{H}\}$, circular dichroism, X-ray data, and/or high-pressure liquid chromatography [14–17]. Among these methods, X-ray data are important to define the absolute configurations of optically active phosphazenes.

On the other hand, phosphazene derivatives with different chemical properties can be utilized in various fields, such as technology, biochemistry, and medicine. Organocyclotriphosphazene derivatives are used as antimicrobial [18] and anticancer [19,20] agents, lubricants [21], flame retardant additives for organic polymers [22], chemosensors [23], and liquid crystals [24].

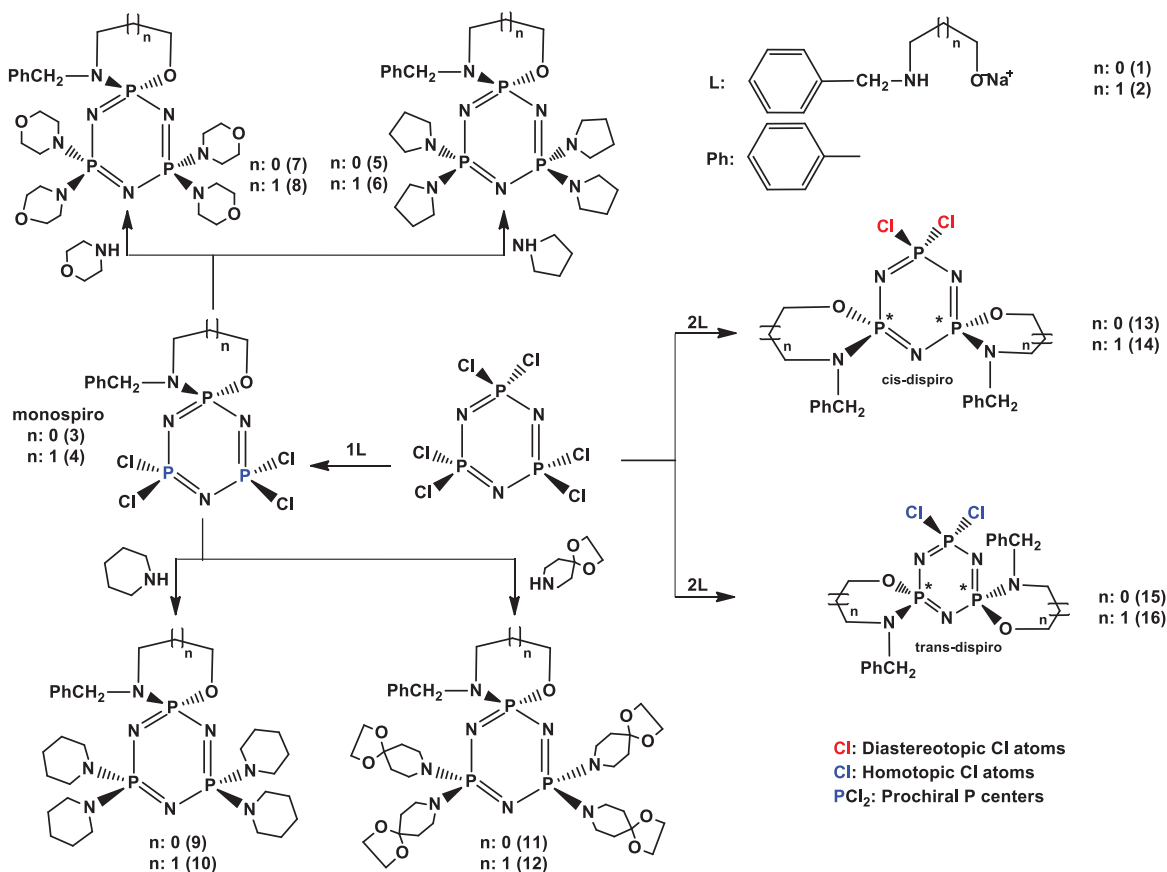
In the literature, some cis- and trans-dispirophosphazene products have been presented, but dispirocyclotriphosphazene derivatives with pendant arms are less common [25,26]. The isomer distributions, chiralities, and structural and spectral features of dispiro products with pendant arms were determined in these studies. In order to compare with the reports in the literature, (N/O) mono- and dispirocyclotriphosphazene derivatives with benzyl pendant arms were prepared in this study. Furthermore, the mono- and dispirocyclotriphosphazene derivatives reported here were also prepared for the determinations of their chemical and biological aspects.

2. Results and discussion

2.1. Synthesis

In synthesis, sodium (N-benzyl)aminopropanoxides **1** and **2** were resynthesized for the preparations of the monospirophosphazenes (**3** and **4**) obtained previously [27], as well as the syntheses of the new cis- and trans-dispirocyclotriphosphazenes (**13–16**). The Cl exchange reactions of 1 equimolar amount of sodium (N-benzyl)aminopropanoxides (**1** and **2**) with 1 equimolar amount of $\text{N}_3\text{P}_3\text{Cl}_6$ afforded the monospirophosphazenes with a benzyl pendant arm (**3** and **4**), according to the literature method. Compounds **3** and **4** possessed 4 exchangeable Cl atoms, owing to the Cl substitution reactions with secondary amines. Hence, tetrakispyrrolidino- (**5** and **6**) [27], morpholino- (**7** and **8**), piperidino- (**9** and **10**), and 1,4-dioxo-8-azaspiro[4,5]decane-(DASD)-phosphazenes (**11** and **12**) were obtained from the reactions of the corresponding monospirophosphazenes (**3** and **4**) with excess amounts of pyrrolidine, morpholine, piperidine, and DASD, respectively. Moreover, the condensations of 1 equimolar amount of $\text{N}_3\text{P}_3\text{Cl}_6$ with 2 equimolar amounts of sodium(N-benzyl)aminopropanoxides (**1** and **2**) yielded monospiro- (**3** and **4**) and cis- and trans-dispirocyclotriphosphazenes (**13–16**) (Scheme). The yields of the mono- (**3** and **4**), cis- (**13** and **14**), and trans-dispiro compounds (**15** and **16**) were 26%, 25%, 30%, 32%, 37%, and 37%, respectively. As understood, the yields of the trans-derivatives were larger than those of the mono- and cis-dispiro products. It could be suggested that the reason for the low yields of the cis-derivatives was the steric interactions between the benzyl groups. THF was used as a solvent in all of the substitution reactions. All of the phosphazene products were purified by column chromatography.

It has already been mentioned that phosphazenes **3–6** were presented in the literature [27]. According to the literature, phosphazenes **3** and **4** were synthesized in THF, while compounds **5** and **6** were synthesized in toluene. However, in the present study, the same compounds (**3–6**) were synthesized in THF. The reaction yields of **3–6** previously reported in the literature were 44%, 55%, 34%, and 45%, respectively [27]. As understood, the reaction yields in this study were higher than those given in the literature. For comparison, the yields of compounds **3–6** can be seen in Section 3.3. Recently, the syntheses of some cis- and trans-spirocyclotriphosphazenes with 4-chloro/4-nitro/4-fluoro-benzyl pendant arms were reported in the literature



Scheme. Replacement reactions of $N_3P_3Cl_6$ with the monodentate and bidentate amines.

[28,29]. Although the trans-geometric isomers of these compounds were purely obtained, the cis-geometric isomers were not isolated from the reaction mixture using crystallization, column chromatography, or preparative TLC. Furthermore, the cis- and trans-isomers of dispirocyclotriphosphazenes with benzyl pendant arms were isolated by column chromatography in this study.

The cis- (**13** and **14**) and trans-phosphazenes (**15** and **16**) possessed 2 stereogenic P atoms, and they were probably present in the meso (RS/SR) and racemic (RR/SS) forms, respectively. As expected, cis-isomer **13** was present as a meso (SR) configuration.

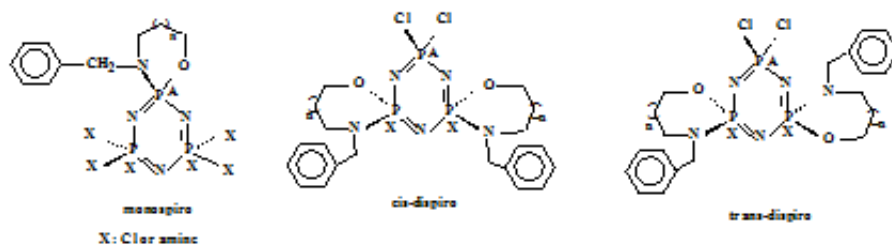
The IR, APIES-MS, NMR, and microanalytical results were consistent with the suggested formulae of the mono- and dispirophosphazene derivatives. Protonated molecular ion peaks ($[MH]^+$) appeared for compounds **7–12**, whereas molecular ion peaks ($[M]^+$) emerged for compounds **13–16** in the mass spectra.

2.2. NMR and IR spectroscopies

The data obtained from the $^{31}P \{^1H\}$ spectra of the mono- (**3–12**) and cis- and trans-dispirophosphazenes (**13–16**) are given in Table 1. The partly and fully substituted monospiro- (**3–12**) and dispirocyclotriphosphazenes (**13–16**) had AX_2 spin systems. A triplet for 1 P atom and a doublet for 2 P atoms were determined in the spectra of the phosphazenes with AX_2 spin systems. Moreover, the cis- and trans-dispiro products (**13–16**)

had a triplet for 1 P atom and a doublet for 2 P (spiro) atoms. The chemical shifts and ${}^2J_{PP}$ values of benzylamino monospirophosphazenes containing 5-membered spiro precursors were larger than those of the other phosphazenes bearing 6-membered spiro-rings. Moreover, the average ${}^2J_{PP}$ constants were 48.4 and 46.2 Hz for the products, including the 5- and 6-membered spiro rings. These findings were inconsistent with the literature data [28,29].

Table 1. ${}^{31}\text{P}$ NMR (decoupled) spectral data of the phosphazenes [chemical shifts (δ) are presented in ppm and J values in Hz]^a.



Compound	Spin system	$\text{P}(\text{Cl})_2$	$\text{P}(\text{NR})_2$	$\text{P}(\text{spiro})$	${}^2J_{PP}$
3	AX_2	24.88 (d)	-	21.03 (t)	52.6
4	AX_2	23.25 (d)	-	9.18 (t)	51.0
5	AX_2	-	19.54 (d)	31.94 (t)	47.0
6	AX_2	-	19.03 (d)	21.28 (t)	45.3
7	AX_2	-	22.59 (d)	31.49 (t)	47.0
8	AX_2	-	21.46 (d)	19.97 (t)	44.7
9	AX_2	-	23.32 (d)	31.80 (t)	47.0
10	AX_2	-	22.23 (d)	20.30 (t)	46.2
11	AX_2	-	22.39 (d)	31.19 (t)	48.6
12	AX_2	-	21.21 (d)	19.79 (t)	43.7
13	AX_2	29.70 (t)	-	27.95 (d)	60.7
14	AX_2	26.73 (t)	-	15.46 (d)	51.0
15	AX_2	30.19 (t)	-	27.71 (d)	60.7
16	AX_2	25.93 (t)	-	15.55 (d)	51.0

The shifts, multiplicities, and coupling constants of the phosphazenes in the ${}^{13}\text{C}$ and ${}^1\text{H}$ spectra were evaluated (Tables S1 and S2). The expected carbon peaks were interpreted using the ${}^{13}\text{C}$ spectra. The carbon peaks of the phenyl rings, C1–C4, were assigned between 125.27 and 138.97 ppm (Table S1). The peaks of the OCH_2 carbons of the spiro rings were between 68.23 and 63.00 ppm. In addition, the signals of the benzylic carbons (PhCH_2) of the products, including the 6-membered spiro rings (**4**, **6**, **8**, **10**, **12**, **14**, and **16**), were shifted further downfield than those of the 5-membered rings (**3**, **5**, **7**, **9**, **11**, **13**, and **15**), as observed previously [28,29]. The same phosphorus atoms, to which 2 heterocyclic groups had bonded, showed 2 groups of NCH_2 , NCH_2CH_2 , $\text{NCH}_2\text{CH}_2\text{CH}_2$, and OCO peaks, with small separations in the ${}^{13}\text{C}$ spectra. Additionally, coupling constants between the C1 and P atoms (${}^3J_{PC}$) emerged in all of the phosphazenes, and the average ${}^3J_{PC}$ value was 8.6 Hz. Coupling constants (${}^2J_{PC}$) of the NCH_2 spiro-groups of the products, including the 5-membered spiro rings (**3**, **5**, **7**, **9**, **11**, **13**, and **15**), were considerably large. The average ${}^2J_{PC}$ value was 12.3 Hz.

The expected proton signals of the phosphazenes were determined from the ^1H spectra (Table S2). The chemical shifts of the aromatic protons (H2, H3, and H4) were in the range of 7.43–7.21 ppm. The δ -values of the PhCH_2N protons of the monospirocyclotriphosphazenes (**3–12**) appeared to be in the range of 4.15–3.86 ppm, like the doublets, due to vicinal coupling with the ^{31}P nucleus. However, the corresponding protons of the dispirocyclotriphosphazenes (**13–16**) had an ABX spin system due to vicinal and geminal couplings with the P atoms and geminal protons, indicating that the 2 geminal protons of the PhCH_2N were diastereotopic. In addition, the $^3\text{J}_{\text{PH}}$ data of the phosphazenes possessing 5-membered spiro rings (**3, 5, 7, 9, 11, 13, and 15**) were slightly smaller than those of the 6-membered rings (**4, 6, 8, 10, 12, 14, and 16**). The average $^3\text{J}_{\text{PH}}$ couplings were 8.1 and 8.3 Hz for the 5- and 6-membered spirophosphazenes. Furthermore, δ -shifts of the NCH_2 and OCH_2 protons of the spiro-precursors were assigned in the ranges of 3.26–2.89 ppm and 4.43–4.21 ppm.

Asymmetric νPN vibrations of the trimeric cyclophosphazenes were assigned in the range of 1200–1172 cm^{-1} in the IR spectra [30]. The aromatic C-H bands were between 3040 cm^{-1} and 3100 cm^{-1} . Moreover, the asymmetric νPCl_2 vibrations of the partly substituted tetra (**3** and **4**) and dichloro phosphazenes (**13–16**) were determined in the range of 562–576 cm^{-1} . These peaks were not observed in the IR spectra of the tetrakis-substituted monospirophosphazene derivatives (**5–12**).

2.3. X-ray structures of compounds **5** and **14**

The crystal structures of compounds **5** and **14** were assigned crystallographically. The crystallographic data of the new products are tabulated in Table 2, and ORTEP diagrams with suitable atom numbering are illustrated in Figures 1 and 2, respectively. Compound **14** had a cis-conformation with respect to the crystallographic results. The trimeric phosphazene skeletons, P1/N1/P2/N2/P3/N3, of compounds **5** and **14** [Figure S1; $\phi_2 = 71.41(2)^\circ$, $\theta_2 = 153.2(8)^\circ$ (for **5**); Figure S2; $\phi_2 = 5.80(1)^\circ$, $\theta_2 = 86.9(1)^\circ$ (for **14**)] were in twisted forms, indicating total puckering amplitudes Q_T of 0.120(2) Å (for **5**) and 0.145(2) Å (for **14**) [31]. As expected, the 5-membered spiro-ring of **5** was in envelope conformation (Figure S3). Both of the spiro-rings of **14** were in chair conformations (Figure S4). Compound **14** crystallized in the P bca space group. The absolute configurations of the P1 and P2 atoms of **14** were determined as S and R, respectively. The shapes of the phosphazene skeletons in **5** and **14** with torsion angles are given in Figure S5, displaying the pseudo mirror plane running from the P1-N1 atoms of the cyclotriphosphazene ring.

Table 3 lists the characteristic bond angles and lengths of **5** and **14**. The exocyclic PN bond lengths were 1.642(2) Å (for **5**), and 1.633(3) and 1.637(2) Å (for **14**), while the endocyclic PN bond lengths were in the ranges of 1.574(2)–1.603(2) Å (for **5**) and 1.554(3)–1.612(3) Å (for **14**). The exocyclic PN bonds were longer than the endocyclic PN bonds. Furthermore, the endocyclic PN bonds were shorter than the PN single bond reported in the literature [32], indicating that the phosphazene ring had nearly double the bond character. Furthermore, regular variations of the bonds in **5** and **14** were also observed, with the distances from P3: P3–N3 \approx P2–N1 > P3–N2 \approx P2–N2 > P1–N1 \approx P1–N3 and P3–N3 \approx P3–N2 ? P2–N1 \approx P1–N1 ? P2–N2 \approx P1–N3.

The endocyclic NPN (α) angles of tetrakis-pyrrolidino monospiro (**5**) and cis-dispirophosphazenes (**14**) [116.27(12) $^\circ$ (for **5**), and 114.20(13) $^\circ$ and 114.95(13) $^\circ$ (for **14**)] were narrow with respect to the values of $\text{N}_3\text{P}_3\text{Cl}_6$, a standard compound [33]. The β and δ (PNP) angles of **5** and **14** were in the ranges of 123.03(13) $^\circ$ –124.43(10) $^\circ$ (for **5**) and 120.57(16) $^\circ$ –125.54(16) $^\circ$ (for **14**) (Table 3). Additionally, it was concluded that the

Table 2. Crystallographic data for compounds **5** and **14**

	5	14
Empirical formula	C ₂₅ H ₄₃ N ₈ P ₃ O	C ₂₀ H ₂₆ N ₅ P ₃ O ₂ Cl ₂
Fw	564.60	532.27
Crystal system	Triclinic	Orthorhombic
Space group	P -1	P bca
<i>a</i> (Å)	10.0618(3)	10.1221(3)
<i>b</i> (Å)	10.1133(3)	18.2196(4)
<i>c</i> (Å)	14.3780(4)	26.5541(5)
α (°)	91.355(2)	90
β (°)	96.254(3)	90
γ (°)	92.965(2)	90
<i>V</i> (Å ³)	1451.79(7)	4897.1(2)
<i>Z</i>	2	8
μ (cm ⁻¹)	0.239 (Mo K α)	0.489 (Mo K α)
ρ (Calc.) (g cm ⁻³)	1.292	1.444
Number of reflections Total	21354	55074
Number of reflections Unique	5111	4334
<i>R</i> _{int}	0.0281	0.0615
$2\theta_{max}$ (°)	50.06	50.14
<i>T</i> _{min} / <i>T</i> _{max}	0.675/0.765	0.8671/0.9391
Number of parameters	334	289
R [F ² >2 σ (F ²)]	0.0522	0.0447
wR	0.1421	0.1051

exocyclic NPO bond angles of these phosphazenes [93.93(11)° (for **5**), 103.03(14)° and 103.43(12)° (for **14**)] were considerably narrow when compared with N₃P₃Cl₆. All of the variations in the bond angles and lengths may be attributed to the steric interactions between the bulky groups and the negative hyperconjugation [34]. When compared with the literature findings, it was clear that the variations in the bond angles and length variations of **5** and **14** were in good agreement with the previously reported data [35].

In addition, the packing diagrams of **5** and **14** are presented in Figures S6 and S7, where the compounds are stacked through the a-axis direction.

2.4. Antimicrobial activity of the compounds

The antibacterial activities of **3–12** and **15** were evaluated against pathogenic bacteria, including 5 strains of G(+) bacteria (*E. hirae*, *E. faecalis*, *B. subtilis*, *B. cereus*, and *S. aureus*) and 6 strains of G(-) bacteria (2 *E. coli* and *K. pneumoniae*, *S. typhimurium*, *P. vulgaris*, and *P. aeruginosa*) using the agar well diffusion method. Evaluation of the antibacterial activities of these compounds is listed in Table S3. The results revealed that compounds **3**, **6**, **7**, **8**, **9**, **11**, **12**, and **15** were effective in suppressing the microbial growth of pathogenic bacteria with variable potency [compound **3** was active against *S. typhimurium* G(-) and *P. vulgaris* G(-); compound **6** against *S. aureus* G(+) and *P. aeruginosa* G(-); compound **7** against *P. aeruginosa* G(-); compound **9**

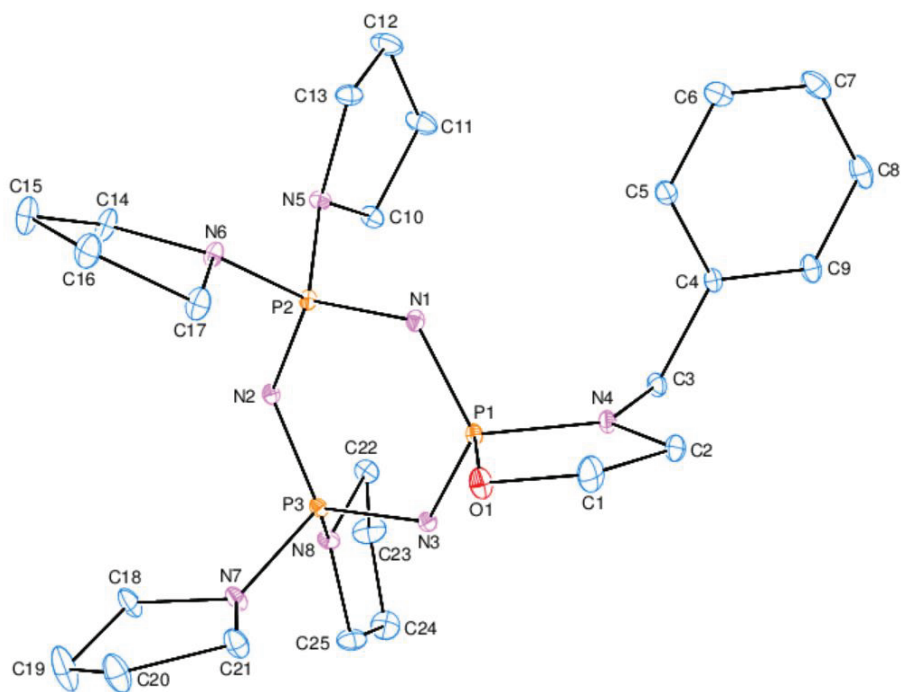


Figure 1. ORTEP-3 drawing of compound **5** with the atom-numbering scheme. Displacement ellipsoids are drawn at the 30% probability level.

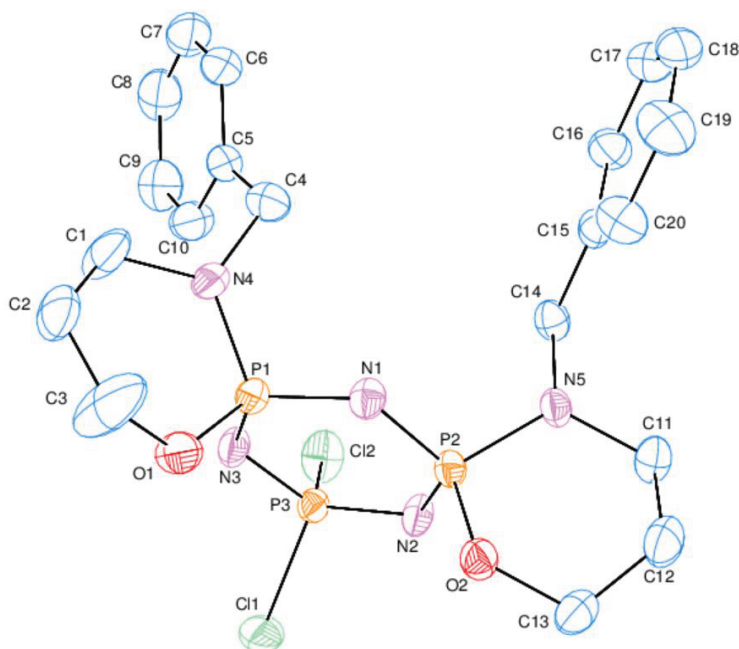


Figure 2. ORTEP-3 drawing of compound **14** with the atom-numbering scheme. Displacement ellipsoids are drawn at the 30% probability level.

Table 3. Selected bond lengths (Å) and angles (deg) for compounds **5** and **14**.

	5	14
P1–N1	1.574(2)	1.579(3)
P1–N3	1.584(2)	1.606(3)
P2–N1	1.600(2)	1.574(3)
P2–N2	1.594(2)	1.612(3)
P3–N2	1.588(2)	1.556(3)
P3–N3	1.603(2)	1.554(3)
P1–N4	1.641(2)	1.633(3)
P1–O1	1.607(2)	1.565(2)
P2–N5	-	1.637(2)
P2–O2	-	1.572(2)
N1–P1–N3 (α)	116.27(12)	114.20(13)
N1–P2–N2 (γ) (α for 14)	115.81(12)	114.95(13)
N2–P3–N3 (γ)	115.85(11)	121.20(14)
P1–N1–P2 (β)	123.98(14)	125.54(16)
P2–N2–P3 (δ)	123.03(13)	120.57(16)
P1–N3–P3 (β)	124.43(10)	121.48(16)
N4–P1–O1 (α')	93.93(11)	103.03(14)
N5–P2–O2 (α')	-	103.43(12)

against *S. aureus* G(+) and *P. aeruginosa* G(-); compound **10** against *P. vulgaris* G(-) and *S. aureus* G(+); compound **11** against *E. hirae* G(+), *P. aeruginosa* G(-), and *P. vulgaris* G(-); and compound **15** against *E. coli* ATCC 25922 G(-), *K. pneumoniae*, *P. vulgaris* G(-), *P. aeruginosa* G(-), *S. aureus* G(+), and *B. subtilis* G(+)]. Compounds **10** and **11** were the most effective at inhibiting microbial growth of the tested bacteria at a concentration of 2500 μ M, whereas compound **15** was effective against several bacterial species. Compounds **6–8** were effective against *P. aeruginosa*. The compounds showed variable antimicrobial activities against fungal strains. Findings of the antimicrobial activities of the products indicated that *E. faecalis* was the bacterium most resistant to the compounds, followed by *E. coli*, whereas *S. aureus*, *S. typhimurium*, and *P. aeruginosa* were the bacteria most susceptible to the compounds. Furthermore, compounds **10**, **11**, and **15** were the most active and exhibited strong antibacterial effects against pathogenic bacteria. It was understood that the pyrrolidino (**6**), piperidino (**9** and **10**), and DASD-substituted benzyl-pendant-armed monospirophosphazenes had activity against G(+) bacteria, while compounds possessing chloro (**3** and **4**) and morpholino (**7** and **8**) had no activity against G(+) bacteria. It appeared that the tetrachloro monospiro (**3**) and dichloro dispiro (**15**) compounds with 5-membered spiro-ring(s) had activity against G(-) bacteria, *S. typhimurium*, *P. vulgaris*, *E. coli* ATCC 25922, and *K. pneumoniae*. According to the minimum inhibitory concentration (MIC) and minimal bacterial concentration (MBC) values, tetrakis-piperidino phosphazene (**9**) was more effective than ampicillin and chloramphenicol against *B. cereus* (G+). Additionally, the tetrakis-pyrrolidino (**6**), morpholino (**7** and **8**), and DASD-substituted (**11**) phosphazenes were very effective against G(-) bacteria (*P. aeruginosa* and *P. vulgaris*).

In addition, compounds **4**, **7**, **8**, **9**, **10**, and **12** showed strong antifungal activity. They exhibited inhibitory effects against *C. krusei* fungus, whereas compound **10** was also effective against *C. tropicalis*. The substituents, i.e. chloro (**4**, six-membered spiro ring), morpholino (**7** and **8**), piperidino (**9** and **10**), and DASD (**12**, six-membered spiro ring), with the exception of pyrrolidino (**5** and **6**) and two-benzyl-pendant-armed dispiro (**15**), played an important role in the activity of the benzyl-pendant-armed monospirophosphazenes.

Experiments were performed to determine their MICs and MBCs against strains of *S. typhimurium*, *P. vulgaris*, *S. aureus*, *P. aeruginosa*, *E. hirae*, *B. cereus*, *C. tropicalis*, and *C. krusei* (Tables 4 and 5). The MICs and MBCs were in the range of 125–500 μM .

Table 4. MIC values of compounds **3**, **4**, and **6–12** on different bacterial and fungal species (in μM) (Amp: ampicillin, C: chloramphenicol (antibacterial), and Keto: ketoconazole (antifungal) used as a control; “-”: the compounds did not cause any growth inhibition; NS: not studied).

Test organisms/ compounds	3	4	6	7	8	9	10	11	12	Amp	C	Keto
<i>E. hirae</i>	-	-	-	-	-	-	-	500	-	< 19.5	156	NS
<i>S. aureus</i>	-	-	250	-	-	-	-	-	-	< 19.5	156	NS
<i>P. aeruginosa</i>	-	-	125	125	125	-	-	125	-	> 2500	> 2500	NS
<i>P. vulgaris</i>	250	-	-	-	250	-	-	250	-	1250	1250	NS
<i>S. typhimurium</i>	250	-	-	-	-	-	-	-	-	< 19.5	156	NS
<i>B. cereus</i>	-	-	-	-	-	125	-	-	-	156	156	NS
<i>C. tropicalis</i>	-	-	-	-	-	-	250	-	-	NS	NS	78
<i>C. krusei</i>	-	250	-	125	125	125	125	-	250	NS	NS	< 19.5

Table 5. MBC and MFC values of compounds **3**, **4**, and **6–12** on different bacterial and fungal species (in μM).

Test organisms/ compounds	3	4	6	7	8	9	10	11	12	Amp	C	Keto
<i>E. hirae</i>	-	-	-	-	-	-	-	1000	-	39	2500	NS
<i>S. aureus</i>	-	-	500	-	-	-	-	-	-	< 19.5	< 19.5	NS
<i>P. aeruginosa</i>	-	-	250	125	250	-	-	125	-	> 2500	> 2500	NS
<i>P. vulgaris</i>	250	-	-	-	250	-	-	250	-	> 2500	2500	NS
<i>S. typhimurium</i>	500	-	-	-	-	-	-	-	-	< 19.5	< 19.5	NS
<i>B. cereus</i>	-	-	-	-	-	125	-	-	-	2500	2500	NS
<i>C. tropicalis</i>	-	-	-	-	-	-	500	-	-	NS	NS	1250
<i>C. krusei</i>	-	500	-	250	250	250	250	-	500	NS	NS	156

Consequently, the antibacterial and antifungal activity results observed in this study were comparable with the literature data. In the literature, pyrrolidino- and DASD-substituted cyclotriphosphazenes containing ferrocenyl/arylspirocyclic pendant arms also had activity against some G(+) and G(-) bacteria and fungi [8,25,26,28,36]. In the present study, the chloro-, pyrrolidino-, morpholino-, piperidino-, and DASD-substituted cyclotriphosphazenes had different antibacterial and fungal activities, as listed in Tables 4 and 5. The antibacterial and antifungal activities of the mono- and dispirocyclotriphosphazene derivatives with benzyl pendant arms could have been due to the formation of hydrogen bonding, dipole-dipole interactions between the DNA of

the bacteria and fungi, or the phosphazene derivatives used in this study. On the other hand, the substituents (chloro, pyrrolidino, DASD, piperidino, and morpholino), the number of members, and the conformations of the spiro rings may also have played an important role in the activity.

2.5. Interactions of DNA with compounds 3–12 and 15

In the present study, 2 DNA bands, namely Forms I and II, appeared for both untreated and treated pBR322 with decreasing concentrations of compounds 6–15 (except for compounds 3, 4, and 15) (Figure 3). In compound 15, a faint, almost coalesced band was observed at 2500 μM (Lane 1), and when the concentrations of the products decreased, the mobility of the bands of Forms I and II increased. The change was less significant with compound 3 at three concentrations, but Form I disappeared at the highest concentration. With compound 4, Forms I and II disappeared at three high concentrations. This was the most damaging compound for the DNA when compared to compound 15. With 15, the separations between the bands were the smallest at 2500–1250 μM (Lanes 1 and 2), below which the separations were larger (Lanes 3 and 4). The presence of a coalesced band suggested a change in the conformation of the DNA of Form I, from the supercoiled Form I to the negative form and from the negative 1 to the positive form [37]. In all of the other compounds, two bands corresponding to Forms I and II were observed in all of the lanes, and a single faint band could be seen in Lanes 2–4 (for 8) and Lane 4 (for 11), corresponding to concentrations of 1250, 625, and 312.5 μM (for 8) and 312.5 μM (for 11), respectively. No bands were observed in Lanes 7 and 8. These bands could have been due to the induced changes in the DNA conformations.

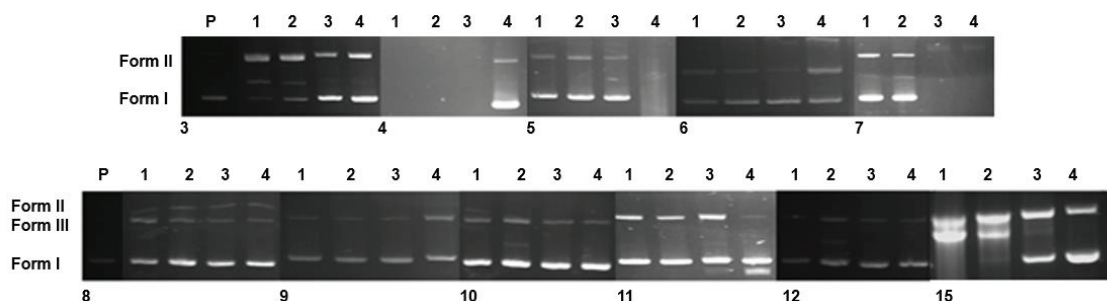


Figure 3. Electrophoretograms of the incubated mixture of pBR322 plasmid DNA and varying concentrations of compounds 3–12 and 15. Lane P: Untreated plasmid DNA. Plasmid DNA of Lanes 1 to 4 interacted with decreasing concentrations of the compounds. Concentrations for the compounds: Lane 1: 2500, Lane: 1250, Lane 3: 625, and Lane 4: 312.5 μM .

3. Experimental

3.1. Reagents used for synthesis

The aliphatic amines (Fluka), ethanolamine, 3-amino-1-propanol, benzaldehyde, and trimer were purchased from Sigma-Aldrich (St. Louis, MO, USA). They were used without further purification. All reactions were followed by TLC using Merck DC Alufolien Kieselgel 60 B254 sheets (Darmstadt, Germany). Merck Kieselgel 60 (230–400 mesh ATSM) silica gel was used for the column chromatography.

3.2. Physical measurements

Microanalytical data were obtained using a LECO CHNS-932 analyzer (St. Joseph, MI, USA). The NMR spectra were supplied on a Bruker DPX FT-NMR (500 MHz) spectrometer (Billerica, MA, USA) (SiMe_4 as

internal and 85% H_3PO_4 as external standards). The spectrometer was equipped with a 5-mm PABBO BB inverse-gradient probe. Standard Bruker pulse programs [38] were used. The IR spectra were obtained on a Mattson 1000 IR spectrometer in KBr disks and were given as cm^{-1} . APIES mass analyses were made on a Waters 2695 Alliance Micromass ZQ spectrometer (Milford, MA, USA).

3.3. Preparations of the compounds

Compounds **1–6** were synthesized according to the literature [27], whereas compounds **1** and **2** were synthesized in ethanol and phosphazenes **3–6** were synthesized in THF.

Compound **3**: Yield: 2.32 g (68%; lit. 44%). mp: 112 °C (lit. 114 °C).

Compound **4**: Yield: 2.29 g (65%; lit. 55%). mp: 110 °C (lit. 110 °C).

Compound **5**: Yield: 0.86 g (66%; lit. 34%). mp: 188 °C (lit. 188 °C).

Compound **6**: Yield: 0.94 g (71%; lit. 45%). mp: 138 °C (lit. 138 °C).

3.3.1. General procedure used for synthesis of the fully-substituted monospirocyclotriphosphazenes (**7–12**)

The solution of heterocyclic amines dissolved in THF (50 mL) was added to the solution of tetrachloromonospirocyclotriphosphazene derivatives in dry THF (100 mL) in the presence of triethylamine (Et_3N). The reactions were refluxed for 24 h by stirring. The crude compounds were separated using column chromatography [toluene and THF (3:1) as eluent]. The phosphazene derivatives were crystallized from petroleum ether (60–80 °C).

Information on synthesis of the fully substituted monospirocyclotriphosphazenes (**7–12**) is given in Table 6.

3.3.2. General procedure used for synthesis of the cis- and trans-dispirocyclotriphosphazenes (**13–16**)

The mixtures of sodium (N-benzyl)aminopropanoxide and Et_3N in THF were added to a stirred solution of $\text{N}_3\text{P}_3\text{Cl}_6$ in THF (50 mL), and stirred and refluxed for 30 h. After the precipitated triethylaminehydrochloride was filtered off, the solvent was evaporated. The three products were purified by column chromatography with toluene and THF (15:1). The first product was the tetrachloro monospirophosphazene derivative. The second product was the cis-dispirocyclotriphosphazene. The last product was the trans-dispirocyclic compound (**15**). The compounds were crystallized from petroleum ether (60–80 °C) at room temperature.

Table 6. Information on the synthesis of the fully-substituted monospirocyclotriphosphazenes (**7–12**).

Tetrachloromonospirocyclotriphosphazene				Heterocyclic amine						Et_3N (mL)	Product	Yield (%)	m.p. (°C)	Rf toluene and THF (2:1)
3		4		Morp.		Pip.		DASD						
G	mmol	g	mmol	mL	mmol	mL	mmol	mL	mmol					
0.80	1.88	-	-	1.94	22.54	-	-	-	-	3	7	68 (0.79 g)	158	0.12
-	-	0.80	1.81	1.88	21.82	-	-	-	-	3	8	70 (0.81 g)	139	0.16
0.80	1.88	-	-	-	-	2.23	22.54	-	-	3	9	72 (0.84 g)	130	0.72
-	-	0.60	1.36	-	-	1.62	16.36	-	-	3	10	73 (0.63 g)	121	0.74
0.80	1.88	-	-	-	-	-	-	2.89	22.56	3	11	79 (1.24 g)	140	0.19
-	-	0.60	1.36	-	-	-	-	2.09	16.32	3	12	81 (0.95 g)	129	0.23

Information on synthesis of the dispirocyclotriphosphazenes (**13–16**) is given in Table 7.

The IR, APIES-MS, and microanalytical data of the products (**7–16**) are tabulated in Table 8.

Table 7. Information on the synthesis of the dispirocyclotriphosphazenes (**13–16**).

Trimer		Comp. 1		Comp. 2		Et ₃ N (mL)	Product	Yield (%)	m.p. (°C)	Rf toluene Êand THF (2:1)
G	mmol	g	mmol	mL	mmol					
4.52	13.00	3.93	26.00	-	-	7.50	3	26 (1.46 g)		
							13	30 (1.97 g)	108	0.70
							15	37 (2.42 g)	114	0.49
3.16	9.09	-	-	3.00	18.18	9.00	4	25 (1.00 g)		
							14	32 (1.55 g)	118	0.72
							16	37 (1.79 g)	124	0.54

3.4. X-ray crystallography

Single crystals of compounds **5** and **14** were grown in acetonitrile at 296 K, and their crystallographic data were collected on a Bruker APEXII CCD area-detector diffractometer by Mo K α . The multiscan absorption correction [39] applied data were processed by SHELX program packages [40,41] for solving and refining the structures, and the ORTEP-3 program [42] was used for the drawings. H atom positions were calculated geometrically at distances of 0.93 and 0.97 Å for methine and methylene, respectively, and refined using a riding model by applying the constraint of 1.2 U_{eq}(carrier atom) for the U_{iso}(H) values.

Determinations of the antimicrobial activities and MIC/MBC/MFC values of the phosphazenes as well as DNA interactions with the compounds were performed according to the method in the literature [43].

4. Conclusion

The present study focused on the syntheses of monospiro (**3–12**) and dispirocyclotriphosphazenes (**13–16**) with benzyl pendant arms. One of the most important aspects of this study was to separate the cis (**13** and **14**) and trans (**15** and **16**) isomers in pure form. The structures of **5** and **14** were determined using X-ray data. The spectral data (¹H, ¹³C, and ³¹P) showed that the structures of all of the compounds were in good agreement with the proposed formulae. The structures of **5** and **14** were symmetric in the solid state with respect to X-ray crystallography. The data showed that the absolute configuration of **14** was SR. In addition, the monospiro (**3** and **4**), cis (meso) (**13** and **14**), and trans (racemic) (**15** and **16**) cyclotriphosphazenes possessed prochiral, diastereotopic, and homotopic atoms. Additionally, most of the compounds were found to inhibit most of the antibacterial activities of bacteria, except for *P. aeruginosa*, *S. aureus*, and *B. cereus*. The antimicrobial activities and MIC values revealed that the most effective compounds were **6–8** and **11**, and the bacterium most affected by the compounds was *P. aeruginosa*. The MBC and MFC values of compounds **3**, **4**, and **6–12** ranged from 250 to 1000 μ M. DNA interaction studies of the cyclotriphosphazenes revealed that compounds **3**, **4**, and **15** had a strong effect on supercoiled DNA by cleavage of the double helix.

In conclusion, the partly tetrachloro monospiro (**3** and **4**) and dichloro dispirocyclotriphosphazenes (**13–16**) could be useful starting compounds for the synthesis of the new organocyclotriphosphazenes as a chiral

Table 8. IR, APIES-MS, and microanalytical data of compounds **7–16**.

Compound	Elemental analyses (%) (Calc./Found)			APIES-MS (Ir %)		IR (ν , KBr, cm^{-1})
	C	H	N	Calc.	Found	
7 ($\text{P}_3\text{N}_8\text{C}_{25}\text{H}_{43}\text{O}_5$)	47.77/47.74	6.90/7.07	17.83/17.45	629	630	3100 (C-H arom.), 2974 (C-H aliph; asymm.), 2902 (C-H aliph; symm.), 1196 (P=N asymm.)
8 ($\text{P}_3\text{N}_8\text{C}_{26}\text{H}_{45}\text{O}_5$)	48.60/48.29	6.74/6.86	17.44/17.13	643	644	3100 (C-H arom.), 2976 (asymm.), 2904 (symm.) (C-H aliph), 1188 (asymm.)
9 ($\text{P}_3\text{N}_8\text{C}_{29}\text{H}_{51}\text{O}$)	56.12/56.42	8.28/8.03	18.05/17.76	621	622	3040 (C-H arom.), 2928 (asymm.), 2830 (symm.) (C-H aliph.), 1186 (asymm.) (P=N)
10 ($\text{P}_3\text{N}_8\text{C}_{30}\text{H}_{53}\text{O}$)	56.77/56.51	8.42/8.09	17.65/17.36	635	636	3080 (C-H arom.), 2972 (asymm.), 2924 (symm.) (C-H aliph.), 1190 (asymm.) (P=N)
11 ($\text{P}_3\text{N}_8\text{C}_{37}\text{H}_{59}\text{O}_9$)	52.11/52.05	6.97/7.02	13.14/12.90	853	854	3100 (C-H arom.), 2972 (asymm.), 2902 (symm.) (C-H aliph), 1200 (asymm.) (P=N)
12 ($\text{P}_3\text{N}_8\text{C}_{38}\text{H}_{61}\text{O}_9$)	52.65/52.41	7.09/7.16	12.93/12.83	867	868	3100 (C-H arom.), 2974 (asymm.), 2906 (symm.) (C-H aliph), 1200 (asymm.)
13 ($\text{C}_{18}\text{H}_{22}\text{N}_5\text{P}_3\text{Cl}_2\text{O}_2$)	42.90/42.81	4.40/4.52	13.90/13.74	503	504	3076 (C-H arom.), 2962 (asymm.), 2902 (symm.) (C-H aliph), 1182 (asymm.) (P=N), 572 (asymm.) (PCl)
14 ($\text{C}_{20}\text{H}_{26}\text{N}_5\text{P}_3\text{Cl}_2\text{O}_2$)	45.13/45.53	4.92/4.59	13.16/13.43	531	532	3088 (C-H arom.), 2968 (asymm.), 2852 (symm.) (C-H aliph), 1172 (asymm.) (P=N), 576 (asymm.) (PCl)
15 ($\text{C}_{18}\text{H}_{22}\text{N}_5\text{P}_3\text{Cl}_2\text{O}_2$)	42.90/42.77	4.40/4.67	13.90/13.80	503	504	3062 (C-H arom.), 2968 (asymm.), 2892 (symm.) (C-H aliph), 1176 (asymm.) (P=N), 566 (asymm.) (PCl)
16 ($\text{C}_{20}\text{H}_{26}\text{N}_5\text{P}_3\text{Cl}_2\text{O}_2$)	45.13/45.22	4.92/4.86	13.16/13.01	531	532	3098 (C-H arom.), 2928 (asymm.), 2906 (symm.) (C-H aliph), 1176 (asymm.) (P=N), 562 (asymm.) (PCl)

catalyst. Additionally, the tetrakis-substituted phosphazenes (**5–12**) are thought to be strong phosphazene bases that can be used as ligating ligands for some metal cations.

Supplementary data

Listings of the ^{13}C (decoupled) and ^1H data of the phosphazenes (Tables S1 and S2), ring conformations, and packing diagrams of compounds **5** and **14** (Figures S1–S4, S6, and S7), shapes of the phosphazene rings in compounds **5** and **14** with torsion angles (Figure S5), and antimicrobial activities, determination of the MIC and MBC/MFC values, and DNA-phosphazene interactions (Section S1) are provided as supplementary information. Crystallographic data for compounds **5** and **14** reported in this paper were deposited with the Cambridge Crystallographic Data Centre, CCDC Nos. 1941517 (for **5**) and 1941518 (for **14**). Copies of the data may be supplied through application to CCDC, 12 Union Road, Cambridge CB2 1EZ, UK. (fax: +44 1223 336033 or e-mail: deposit@ccdc.cam.ac.uk or at <http://www.ccdc.cam.ac.uk>).

Acknowledgments

The authors thank TÜBİTAK (Scientific and Technical Research Council of Turkey, Grant No: 116Z400). Z.K. is grateful the Turkish Academy of Sciences (TÜBA) for partial support of this work. T.H. acknowledges the Hacettepe University Scientific Research Project Unit (Grant No: 013 D04 602 004).

References

1. Allen CW. Linear, cyclic and polymeric phosphazenes. *Coordination Chemistry Reviews* 1994; 130: 137-173.
2. Chandrasekhar V, Chakraborty A. *Organophosphorus Chemistry*. London, UK: Royal Society of Chemistry, 2019.
3. Allen CW. Regio- and stereochemical control in substitution reactions of cyclophosphazenes. *Chemical Reviews* 1991; 91: 119-135.
4. Stewart FF. *Organophosphorus Chemistry*. London, UK: Royal Society of Chemistry, pp. 397-430.
5. Asmafiliz N, İter EE, Kılıç Z, Hökelek T, Şahin E. Phosphorus-nitrogen compounds: Part 15. Synthesis, anisochromism and the relationship between crystallographic and spectral data of monotopic *spiro*-crypta phosphazenes. *Journal of Chemical Sciences* 2008; 120: 363-376.
6. Jaeger R, Gleria M. Poly(organophosphazene)s and related compounds: Synthesis, properties and applications. *Progress in Polymer Science* 1998; 23: 179-276.
7. Gleria M, Jaeger R. de. *Phosphazenes: A Worldwide Insight*. New York, NY, USA: Nova Publishers, 2004.
8. Asmafiliz N, Kılıç Z, Öztürk A, Hökelek T, Koç LY et al. Phosphorus-nitrogen compounds. 18. Syntheses, stereogenic properties, structural and electrochemical investigations, biological activities, and DNA interactions of new spirocyclic mono- and bisferrocenylphosphazene derivatives. *Inorganic Chemistry* 2009; 48: 10102-10116.
9. Uslu A, Yeşilot S. Chiral configurations in cyclophosphazene chemistry. *Coordination Chemistry Reviews* 2015; 291: 28-67.
10. Kumar NS, Kumara Swamy KC. Synthesis and structures of unsymmetrical bis- and tris-cyclotriphosphazenes. *Polyhedron* 2004; 23: 979-985.
11. İter EE, Asmafiliz N, Işıklan M, Kılıç Z, Çaylak N et al. Phosphorus-nitrogen compounds. 14. Synthesis, stereogenicity, and structural investigations of novel N/O spirocyclic phosphazene derivatives. *Inorganic Chemistry* 2007; 46 (23): 9931-9944.
12. Tümer Y, Asmafiliz N, Zeyrek CT, Kılıç Z, Açıık L et al. Syntheses, spectroscopic and crystallographic characterizations of cis- and trans-dispirocyclic ferrocenylphosphazenes: molecular dockings, cytotoxic and antimicrobial activities. *New Journal of Chemistry* 2018; 42 (3): 1740-1756.

13. Tümer Y, Asmafiliz N, Kılıç Z, Aydın B, Açık L et al. Phosphorus-nitrogen compounds: Part 43. Syntheses, spectroscopic characterizations and antimicrobial activities of cis- and trans-N/O dispirocyclotriphosphazenes containing ferrocenyl pendant arms. *Journal of Molecular Structure* 2018; 1173: 885-893.
14. Beşli S, Allen CW, Mutlu Balcı C, Kara G, Yeşilot S et al. Stereochemical aspects of cyclotriphosphazenes: Prochiral and pseudo-asymmetric phosphorus atoms. *Polyhedron* 2017; 135: 49-59.
15. Kajiyama K, Setone Y, Aoyagi K, Yuge H. Chiral HPLC separations, absolute structural elucidation, and determination of stereochemical stability of trans-bis[2-(2-pyridinyl)aminophenolato]cyclotriphosphazene. *Chirality* 2016; 556-561.
16. Bui TTT, Coles SJ, Davies DB, Drake AF, Eaton RJ et al. Chiral separation and CD characterisation of enantiomeric cyclotriphosphazene derivatives. *Chirality* 2005; 17: 438-443.
17. Asmafiliz N. Syntheses of chiral phosphazenes with stereogenic centers: NMR behavior in the presence of a chiral solvating agent. *Heteroatom Chemistry* 2014; 25: 83-94.
18. Akbaş H, Okumuş A, Kılıç Z, Hökelek T, Süzen Y et al. Phosphorus-nitrogen compounds part 27. Syntheses, structural characterizations, antimicrobial and cytotoxic activities, and DNA interactions of new phosphazenes bearing secondary amino and pendant (4-fluorobenzyl)spiro groups. *European Journal of Medicinal Chemistry* 2013; 70: 294-307.
19. Görgülü AO, Koran K, Özen F, Tekin S, Sandal S. Synthesis, structural characterization and anti-carcinogenic activity of new cyclotriphosphazenes containing dioxybiphenyl and chalcone groups. *Journal of Molecular Structure* 2015; 1087: 1-10.
20. Bartel C, Bytzek AK, Scaffidi-Domianello YY, Grabmann G, Jakupec MA et al. Cellular accumulation and DNA interaction studies of cytotoxic trans-platinum anticancer compounds. *Journal of Biological Inorganic Chemistry* 2012; 17: 465-474.
21. Zhu J, Liu W, Chu R, Meng X. Tribological properties of linear phosphazene oligomers as lubricants. *Tribology International* 2007; 40: 10-12.
22. Lv M, Yao C, Yang D, Zeng H. Synthesis of a melamine-cyclotriphosphazene derivative and its application as flame retardant on cotton gauze. *Journal of Applied Polymer Science* 2016; 133 (25): 43555.
23. Şenkuytu E, Tanrıverdi Eçik E. Octa-BODIPY derivative dendrimeric cyclotetraphosphazenes; photophysical properties and fluorescent chemosensor for Co^{2+} ions. *Spectrochimica Acta Part A: Molecular and Biomolecular Spectroscopy* 2017; 173: 863-870.
24. Barbera J, Bardaj M, Jimnez J, Laguna A, Martnez J et al. Columnar mesomorphic organizations in cyclotriphosphazenes. *Journal of the American Chemical Society* 2005; 127: 8994-9002.
25. Okumuş A, Akbaş H, Kılıç Z, Koç LY, Açık L et al. Phosphorus-nitrogen compounds part 33: in vitro cytotoxic and antimicrobial activities, DNA interactions, syntheses, and structural investigations of new mono(4-nitrobenzyl)spirocyclotriphosphazenes. *Research on Chemical Intermediates* 2016; 42: 4221-4251.
26. Asmafiliz N, Civan M, Özben A, Kılıç Z, Ramazanoğlu N et al. Phosphorus-nitrogen compounds. Part 39. Syntheses and Langmuir-Blodgett thin films and antimicrobial activities of N/N and N/O spirocyclotriphosphazenes with monoferrocenyl pendant arm. *Applied Organometallic Chemistry* 2018; 32 (4): e-4223.
27. Coşkun S. N/O Donörlü spiro halkalı fosfazene bileşiklerinin sentezi, stereojenik, spektroskopikve kristallografik özelliklerinin incelenmesi. MSc, Kırıkkale University, Kırıkkale, Turkey, 2011 (in Turkish).
28. Asmafiliz N, Berberoğlu İ, Özgür M, Kılıç Z, Kayalak H et al. Phosphorus-nitrogen compounds: Part 46. The reactions of $\text{N}_3\text{P}_3\text{Cl}_6$ with bidentate and monodentate ligands: The syntheses, structural characterizations, antimicrobial and cytotoxic activities, and DNA interactions of (N/N)spirocyclotriphosphazenes with 4-chlorobenzyl pendant arm. *Inorganica Chimica Acta* 2019; 495: 118949.

29. Tanrıkulu Gİ, Yakut Özgür M, Okumuş A, Kılıç Z, Hökelek T et al. Phosphorus-Nitrogen compounds part 47: The conventional and microwave-assisted syntheses of dispirocyclotriphosphazene derivatives with (4-fluoro/4-nitrobenzyl) pendant arms: Structural and stereogenic properties and DNA interactions. *Inorganica Chimica Acta* 2019; 490: 179-189.
30. Carriedo GA, Alonso FG, Gonzalez PA, Menendez JR. Infrared and Raman spectra of the phosphazene high polymer $[NP(O_2C_{12}H_8)]_n$. *Journal of Raman Spectroscopy* 1998; 29: 327-330.
31. Cremer D, Pople JA. Molecular orbital theory of the electronic structure of organic compounds. XXIII. Pseudorotation in saturated five-membered ring compounds. *Journal of the American Chemical Society* 1975; 97: 1354-1358.
32. Allen FH, Kennard O, Watson DG, Brammer L, Orpen AG et al. Tables of bond lengths determined by X-ray and neutron diffraction. Part 1. Bond lengths in organic compounds. *Journal of the Chemical Society, Perkin Transactions 2* 1987; 1-19
33. Bullen GJ. An improved determination of the crystal structure of hexachlorocyclotriphosphazene (phosphonitrilic chloride). *Journal of the Chemical Society A: Inorganic, Physical, Theoretical* 1971; 1450-1453.
34. Chaplin AB, Harrison JA, Dyson PJ. Revisiting the electronic structure of phosphazenes. *Inorganic Chemistry* 2005; 44: 8407-8417.
35. Tümer Y, Asmafiliz N, Kılıç Z, Hökelek T, Koç LY et al. Phosphorus-nitrogen compounds: Part 28. Syntheses, structural characterizations, antimicrobial and cytotoxic activities, and DNA interactions of new phosphazenes bearing vanillinato and pendant ferrocenyl groups. *Journal of Molecular Structure* 2013; 1049: 112-124.
36. Asmafiliz N, Kılıç Z, Hökelek T, Koç LY, Açık L et al. Phosphorus–nitrogen compounds: Part 26. Syntheses, spectroscopic and structural investigations, biological and cytotoxic activities, and DNA interactions of mono and bisferrocenylspirocyclotriphosphazenes. *Inorganica Chimica Acta* 2013; 400: 250-261.
37. Daghriria H, Huqa F, Beal P. Studies on activities, cell up take and DNA binding of four multinuclear complexes of the form: $[\{trans-PtCl(NH_3)_2\}_2\mu-\{trans-Pd(NH_3)_2-(H_2N(CH_2)_nNH_2)_2\}]Cl_4$ where $n = 4-7$. *Journal of Inorganic Biochemistry* 2004; 98: 1722-1733.
38. Bruker Inc. Program 1D WIN-NMR (Release 6.0) and 2D WIN-NMR (Release 6.1). Madison, WI, USA: Bruker, 2005.
39. Bruker Inc. SADABS. Madison, WI, USA: Bruker, 2005.
40. Sheldrick GM. SHELXS-97, SHELXL-97. Göttingen, Germany: University of Göttingen, 1997.
41. Sheldrick GM. A short history of SHELX. *Acta Crystallographica Section A: Foundations and Advances* 2008; 64: 112-122.
42. Farrugia LJ. *ORTEP-3* for Windows – A version of ORTEP-III with a graphical user interface (GUI). *Journal of Applied Crystallography* 1997; 30: 565-566.
43. Berberoğlu İ, Asmafiliz N, Kılıç Z, Hökelek T, Koç LY et al. Phosphorus nitrogen compounds: Part 34. Syntheses, structural investigations, cytotoxic and biological activities of spiro-ansa-spiro and spiro-bino-spiro tetrameric phosphazene derivatives. *Inorganica Chimica Acta* 2016; 446: 75-86.

Supplementary information

Table S1. ^{13}C (decoupled) NMR spectral data of the phosphazenes. Chemical shifts (δ) reported in ppm and J values in Hz.

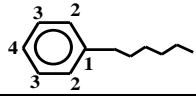
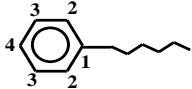
	3	4	5	6	7	8	9	10	11	12	13	14	15	16
														
$\text{NCH}_2\text{CH}_2\text{CH}_2$	-	-	-	-	-	-	25.00 25.08	25.04 25.16	-	-	-	-	-	-
NCH_2CH_2	-	25.88 $^3J_{\text{PC}} = 4.6$	26.30 $^3J_{\text{PC}} = 9.9$ 26.35 $^3J_{\text{PC}} = 9.9$ (pyrr)	26.62 $^3J_{\text{PC}} = 3.0$ (spiro) 26.30 $^3J_{\text{PC}} = 7.6$ 26.35 $^3J_{\text{PC}} = 8.4$ (pyrr)	-	26.52 $^3J_{\text{PC}} = 3.0$ (spiro)	26.29 $^3J_{\text{PC}} = 7.6$ 26.36 $^3J_{\text{PC}} = 8.1$ (pip)	26.65 $^3J_{\text{PC}} = 3.8$ (spiro) 26.35 $^3J_{\text{PC}} = 8.4$ 26.39 $^3J_{\text{PC}} = 7.6$ (pip)	35.45 $^3J_{\text{PC}} = 6.8$ $^3J_{\text{PC}} = 6.8$ (DASD)	26.61 (spiro) 35.49 $^3J_{\text{PC}} = 6.8$ 35.60 $^3J_{\text{PC}} = 6.1$ (DASD)	-	26.17 $^3J_{\text{PC}} = 7.0$	-	26.20
NCH_2	45.90 $^2J_{\text{PC}} = 17.5$	45.46	46.52 $^2J_{\text{PC}} = 15.2$ (spiro) 46.07 $^2J_{\text{PC}} = 4.6$ 46.15 (pyrr)	45.98 (spiro) 46.04 $^2J_{\text{PC}} = 4.6$ 46.23 $^2J_{\text{PC}} = 4.6$ (pyrr)	46.65 $^2J_{\text{PC}} = 15.2$ (spiro) 44.56 (mor)	45.98 (spiro) 44.63 44.75 (mor)	46.50 $^2J_{\text{PC}} = 14.5$ (spiro) 45.17 45.32 (pip)	46.09 (spiro) 45.24 45.43 (pip)	46.15 $^2J_{\text{PC}} = 14.5$ (spiro) 42.53 42.59 (DASD)	45.96 (spiro) 42.61 42.68 (DASD)	46.05 $^2J_{\text{PC}} = 8.3$ 46.13 $^2J_{\text{PC}} = 8.3$	45.47 45.69	46.04 $^2J_{\text{PC}} = 8.6$ 46.16 $^2J_{\text{PC}} = 8.4$	45.47
OCH_2	65.58	68.23 $^2J_{\text{PC}} = 7.6$	63.00	63.87 $^2J_{\text{PC}} = 6.9$	63.40 $^3J_{\text{PC}} = 6.8$ (spiro) 67.15 $^3J_{\text{PC}} = 7.6$ (mor)	66.30 $^3J_{\text{PC}} = 6.8$ (spiro) 67.24 $^3J_{\text{PC}} = 8.4$ (mor)	63.09	65.89 $^2J_{\text{PC}} = 6.9$	63.17 (spiro) 64.16 (DASD)	66.06 $^2J_{\text{PC}} = 6.8$ (spiro) 64.16 (DASD)	64.82	67.44 67.47	64.84	67.46
PhCH_2	48.01 $^2J_{\text{PC}} = 6.1$	51.03 $^2J_{\text{PC}} = 3.1$	48.62 $^2J_{\text{PC}} = 6.8$	52.05 $^2J_{\text{PC}} = 1.5$	49.21 $^2J_{\text{PC}} = 6.1$	51.93	49.51 $^2J_{\text{PC}} = 6.1$	52.11	49.24 $^2J_{\text{PC}} = 6.1$	51.86	48.25 $^2J_{\text{PC}} = 3.2$ 48.27 $^2J_{\text{PC}} = 2.6$	51.10 51.30	48.32 $^2J_{\text{PC}} = 3.1$ 48.28 $^2J_{\text{PC}} = 3.0$	51.10
OCO	-	-	-	-	-	-	-	-	107.46 107.64 (DASD)	107.57 107.78 (DASD)	-	-	-	-
C4	127.98	127.79	128.37	126.80	125.27	127.23	127.02	126.80	127.06	126.87	127.61	127.33	127.60	127.34
C3	128.20	128.54	129.45	128.04	127.77	128.33	128.11	128.06	128.10	128.11	127.98	128.34 128.37	127.95	128.37
C2	128.78	128.61	132.74	128.71	128.49	128.37	128.25	128.67	128.30	128.64	128.57	128.64	128.62	128.65
C1	136.14 $^3J_{\text{PC}} = 6.1$	136.20 $^3J_{\text{PC}} = 9.1$	137.49 $^3J_{\text{PC}} = 6.6$	138.97 $^3J_{\text{PC}} = 10.6$	137.99 $^3J_{\text{PC}} = 7.6$	137.99 $^3J_{\text{PC}} = 10.6$	138.84 $^3J_{\text{PC}} = 8.4$	138.91 $^3J_{\text{PC}} = 9.6$	138.34 $^3J_{\text{PC}} = 7.7$	138.36 $^3J_{\text{PC}} = 10.7$	136.90 $^3J_{\text{PC}} = 7.0$	137.11 137.28 $^3J_{\text{PC}} = 9.9$	136.89 $^3J_{\text{PC}} = 6.9$	137.11 137.28 $^3J_{\text{PC}} = 9.1$

Table S2. ¹H NMR spectral data of the phosphazenes. Chemical shifts (δ) reported in ppm and *J* values in Hz. d: Doublet, m: multiplet, t: triplet and dd: doublet of doublets.

	3	4	5	6	7	8	9	10	11	12	13	14	15	16
NCH ₂ CH ₂ CH ₂	–	–	–	–	–	–	1.44 (m, 4H) 1.50 (m, 4H)	1.43–1.55 (m, 8H)	–	–	–	–	–	–
NCH ₂ CH ₂	–	1.93 (m, 2H) ³ J _{HH} = 6.0 ³ J _{HH} = 6.0	1.72 (m, 8H) 1.77 (m, 8H) (pyrr)	1.67–1.79 (m, 2H) ³ J _{HH} = 6.0 1.67–1.79 (m, 16H) (pyrr)	–	1.82 (m, 2H) ³ J _{HH} = 6.0	1.79 (m, 16H)	1.79 (m, 2H) ³ J _{HH} = 5.2 (spiro) 1.43–1.55 (m, 16H)	1.61 (m, 8H) 1.67 (m, 8H) ³ J _{HH} = 6.0	1.77 (m, 2H) ³ J _{HH} = 5.2 ³ J _{HH} = 6.4 (spiro) 1.57 (m, 8H) ³ J _{HH} = 6.4 1.65 (m, 8H) ³ J _{HH} = 5.2 (DASD)	–	1.80 (m, 2H) ³ J _{HH} = 4.4 ³ J _{HH} = 4.8 1.80 (m, 2H) ³ J _{HH} = 4.4 ³ J _{HH} = 4.8	–	1.80 (m, 2H) ³ J _{HH} = 5.2 ³ J _{HH} = 6.0 1.95 (m, 2H) ³ J _{HH} = 5.5 ³ J _{HH} = 6.0
NCH ₂	3.26 (m, 2H) ³ J _{HH} = 6.5 ³ J _{PH} = 10.8	3.07 (m, 2H) ³ J _{HH} = 6.0 ³ J _{PH} = 11.6	3.03–3.15 (m, 2H) ³ J _{HH} = 6.0 (spiro) 3.03–3.15 (m, 16H) (pyrr)	2.91 (m, 2H) ³ J _{HH} = 5.6 ³ J _{PH} = 12.0 (spiro) 2.97–3.18 (m, 16H) (pyrr)	3.07–3.20 (m, 2H) ³ J _{HH} = 6.4 (spiro) 3.07–3.20 (m, 16H) ³ J _{HH} = 4.4 ³ J _{HH} = 4.4 (mor)	2.95 (m, 2H) ³ J _{HH} = 6.2 ³ J _{PH} = 13.6 (spiro) 3.03–3.15 (m, 16H) ³ J _{HH} = 5.8 ³ J _{HH} = 6.8 (mor)	2.92 (m, 2H) ³ J _{HH} = 5.6 ³ J _{PH} = 13.6 (spiro) 3.01–3.07 (m, 16H) (pip)	2.89–3.07 (m, 2H) ³ J _{HH} = 5.2 (spiro) 2.89–3.07 (m, 16H) (pip)	3.11–3.20 (m, 2H) ³ J _{HH} = 6.8 (spiro) 3.11–3.20 (m, 16H) ³ J _{HH} = 5.2 ³ J _{HH} = 6.0 (DASD)	2.91 (m, 2H) ³ J _{HH} = 6.4 ³ J _{PH} = 11.6 (spiro) 3.10–3.24 (m, 16H) ³ J _{HH} = 5.2 ³ J _{HH} = 6.4 (DASD)	3.23 (m, 4H) ³ J _{HH} = 6.4 ³ J _{PH} = 11.6	3.03 (m, 4H) ³ J _{HH} = 4.8 ³ J _{PH} = 9.6	3.37 (m, 4H) ³ J _{HH} = 6.0 ³ J _{PH} = 10.8	3.03 (m, 4H) ³ J _{HH} = 6.0
OCH ₂	4.36 (m, 2H) ³ J _{HH} = 6.5 ³ J _{PH} = 10.8	4.41 (m, 2H) ³ J _{HH} = 6.0 ³ J _{PH} = 10.8	4.21 (m, 2H) ³ J _{HH} = 6.0 ³ J _{PH} = 10.0	4.27 (m, 2H) ³ J _{HH} = 6.0 ³ J _{PH} = 10.8	4.22 (m, 2H) ³ J _{HH} = 6.4 ³ J _{PH} = 9.6 (spiro) 3.57	4.28 (m, 2H) ³ J _{HH} = 6.0 ³ J _{PH} = 12.8 (spiro) 3.55	4.28 (m, 2H) ³ J _{HH} = 5.2 ³ J _{PH} = 7.6	4.28 (m, 2H) ³ J _{HH} = 5.2 ³ J _{PH} = 10.8	4.22 (m, 2H) ³ J _{HH} = 6.8 ³ J _{PH} = 9.2 (spiro) 3.91	4.24 (m, 2H) ³ J _{HH} = 5.2 ³ J _{PH} = 10.8 (spiro) 3.89	4.40 (m, 4H) ³ J _{HH} = 6.4 ³ J _{PH} = 11.2	4.43 (m, 4H) ³ J _{HH} = 4.4	4.33 (m, 4H) ³ J _{HH} = 6.0 ³ J _{PH} = 7.6	4.43 (m, 4H) ³ J _{HH} = 6.0

					(t, 8H) $^3J_{HH} = 4.4$ 3.64 (t, 8H) $^3J_{HH} = 4.4$ (mor)	(t, 8H) $^3J_{HH} = 6.8$ 3.64 (t, 8H) $^3J_{HH} = 5.8$ (mor)			(s, 8H) 3.94 (s, 8H)	(s, 8H) 3.92 (s, 8H) (DASD)				
PhCH ₂	4.10 (d, 2H) $^3J_{PH} = 10.0$	3.98 (d,2H) $^3J_{PH} = 8.0$	4.01 (d, 2H) $^3J_{PH} = 8.4$	3.94 (d, 2H) $^3J_{PH} = 6.8$	4.04 (d, 2H) $^3J_{PH} = 7.2$	3.90 (d, 2H) $^3J_{PH} = 6.8$	3.92 (d, 2H) $^3J_{PH} = 7.2$	3.92 (d, 2H) $^3J_{PH} = 7.2$	4.00 (d, 2H) $^3J_{PH} = 6.8$	3.86 (d, 2H) $^3J_{PH} = 6.8$	3.87 (d, 2H) $^3J_{PH} = 8.4$ 4.00 (d, 2H) $^3J_{PH} = 8.4$	3.86 (dd, 1H) $^2J_{HH} = 12.8$ $^3J_{PH} = 8.8$ 3.87 (dd, 1H) $^2J_{HH} = 12.8$ $^3J_{PH} = 9.2$ 4.04 (dd, 1H) $^2J_{HH} = 14.4$ $^3J_{PH} = 9.6$ 4.13 (dd, 1H) $^2J_{HH} = 14.4$ $^3J_{PH} = 10.0$	3.99 (d, 2H) $^3J_{PH} = 8.0$ 4.04 (d, 2H) $^3J_{PH} = 8.4$	3.86 (dd, 2H) $^2J_{HH} = 14.4$ $^3J_{PH} = 7.2$ 3.89 (dd, 2H) $^2J_{HH} = 14.4$ $^3J_{PH} = 7.2$ 4.11 (dd, 1H) $^2J_{HH} = 14.4$ $^3J_{PH} = 10.0$ 4.15 (dd, 1H) $^2J_{HH} = 14.4$ $^3J_{PH} = 10.0$
H4	7.29–7.42 (1H)	7.30–7.40 (1H)	7.27 (1H)	7.21 (t, 1H) $^3J_{HH} = 7.6$	7.31 (t, 1H) $^3J_{HH} = 7.2$	7.25 (t, 1H) $^3J_{HH} = 5.6$	7.22 (t, 1H) $^3J_{HH} = 6.8$	7.23 (t, 1H) $^3J_{HH} = 6.8$	7.23 (t, 1H) $^3J_{HH} = 7.6$	7.21 (t, 1H) $^3J_{HH} = 7.8$	7.22–7.43 (2H)	7.21–7.42 (2H)	7.24–7.43 (2H)	7.28 (t, 2H) $^3J_{HH} = 7.6$
H3	7.29–7.42 (2H)	7.30–7.40 (2H)	7.25 $^3J_{HH} = 8.4$ (d,2H)	7.28 (dd, 2H) $^3J_{HH} = 7.6$ $^3J_{HH} = 7.6$	7.24 (dd, 2H) $^3J_{HH} = 7.6$ $^3J_{HH} = 7.2$	7.30 (dd, 2H) $^3J_{HH} = 7.4$ $^3J_{HH} = 5.6$	7.29 (dd, 2H) $^3J_{HH} = 6.8$ $^3J_{HH} = 7.4$	7.29 (dd, 2H) $^3J_{HH} = 6.8$ $^3J_{HH} = 7.2$	7.30 (dd, 2H) $^3J_{HH} = 7.6$ $^3J_{HH} = 7.6$	7.27 (dd, 2H) $^3J_{HH} = 7.8$ $^3J_{HH} = 7.2$	7.22–7.43 (4H)	7.21–7.42 (4H)	7.24–7.43 (4H)	7.35 (dd, 4H) $^3J_{HH} = 7.2$ $^3J_{HH} = 7.6$
H2	7.29–7.42 (2H)	7.30–7.40 (2H)	7.40 $^3J_{HH} = 8.4$ (d,2H)	7.41 (d, 1H) $^3J_{HH} = 7.6$	7.40 (d, 1H) $^3J_{HH} = 7.6$	7.38 (d, 1H) $^3J_{HH} = 7.4$	7.42 (d, 1H) $^3J_{HH} = 7.4$	7.42 (d, 1H) $^3J_{HH} = 7.2$	7.41 (d, 1H) $^3J_{HH} = 7.6$	7.37 (d, 1H) $^3J_{HH} = 7.2$	7.22–7.43 (4H)	7.21–7.42 (4H)	7.24–7.43 (4H)	7.41 (d, 4H) $^3J_{HH} = 7.2$

Table S3. Antimicrobial activities of compounds **3–12** and **15** on different bacterial and fungal strains. The inhibition zones diameters of the compounds are expressed in mm. Amp: Ampicillin, C: chloramphenicol (antibacterial), and Keto: ketoconazole (antifungal) used as a control; “-”: the compounds did not cause any growth inhibition; NS: not studied.

Test organisms/ Compounds	3	4	5	6	7	8	9	10	11	12	15	Amp	C	Keto
<i>E. coli</i> ATCC 25922 G(-)	-	-	-	-	-	-	-	-	-	-	13.0 ± 1.0	18.0 ± 0.0	25.0 ± 0.0	NS
<i>E. coli</i> ATCC 35218 G(-)	-	-	-	-	-	-	-	-	-	-	-	-	8.0 ± 0.0	NS
<i>E. hirae</i> ATCC 9790 G(+)	-	-	-	-	-	-	-	-	20.3 ± 0.5	-	-	9.0 ± 1.0	22.0 ± 1.0	NS
<i>E. faecalis</i> ATCC 29212 G(+)	-	-	-	-	-	-	-	-	-	-	-	27.0 ± 1.0	20.0 ± 0.0	NS
<i>K. pneumoniae</i> ATCC 13883 G(-)	-	-	-	-	-	-	-	-	-	-	13.0 ± 1.0	-	31.0 ± 1.0	NS
<i>P. aeruginosa</i> ATCC 27853 G(-)	-	-	-	21.7 ± 0.9	16.7 ± 0.9	15.0 ± 1.0	-	-	16.0 ± 0.8	-	12.0 ± 1.0	60.0 ± 0.0	34.0 ± 0.0	NS
<i>P. vulgaris</i> RSKK 96029 G(-)	15.0 ± 0.0	-	-	-	-	-	-	16.0 ± 1.0	15.7 ± 0.5	-	12.0 ± 1.0	-	32.0 ± 1.0	NS
<i>S. typhimurium</i> ATCC 14028 G(-)	16.7 ± 0.5	-	-	-	-	-	-	-	-	-	-	19.0 ± 1.0	38.0 ± 1.0	NS

<i>S. aureus</i> G(+) ATCC 25923	-	-	-	15.5 ± 0.5	-	-	13.0 ± 0.8	12.7 ± 0.5	-	-	11.0 ± 0.0	44.0 ± 1.0	24.0 ± 1.0	NS
<i>B. subtilis</i> ATCC 6633 G(+)	-	-	-	-	-	-	-	-	-	-	11.0 ± 1.0	23.0 ± 1.0	21.0 ± 0.0	NS
<i>B. cereus</i> NRRL B-3711 G(+)	-	-	-	-	-	-	15.0 ± 0.0	-	-	-	-	-	-	NS
<i>C. tropicalis</i> ATCC 10231	-	-	-	-	-	-	-	20.0 ± 0.0	-	-	-	NS	NS	34.0 ± 2.0
<i>C. albicans</i> ATCC 10231	-	-	-	-	-	-	-	-	-	-	-	NS	NS	11.0 ± 1.0
<i>C. krusei</i> ATCC 6258	-	14.7 ± 0.9	-	-	15.7 ± 0.5	16.3 ± 0.5	16.3 ± 0.5	15.0 ± 1.0	-	14.5 ± 0.5	-	NS	NS	18.0 ± 1.0



Figure S1. The conformations of the phosphazene ring of **5**.



Figure S2. The conformations of the phosphazene ring of **14**.

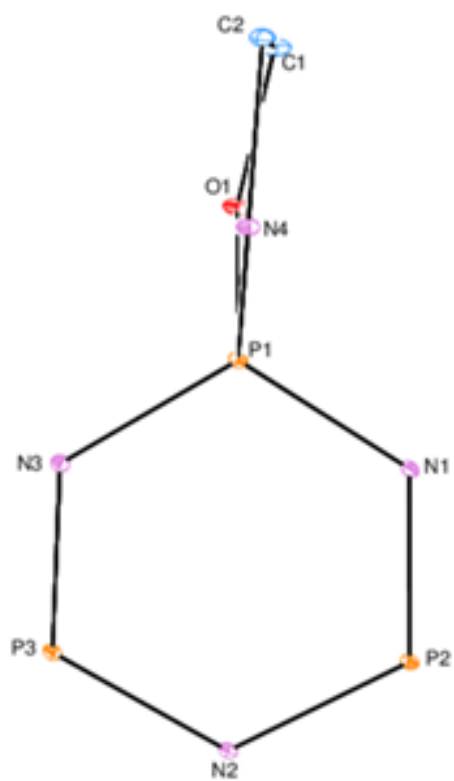
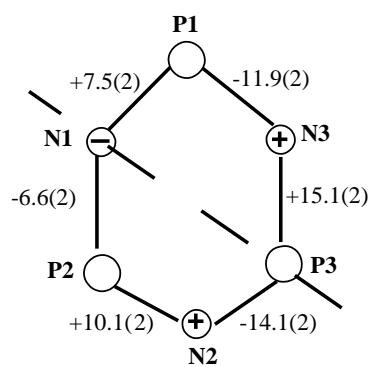


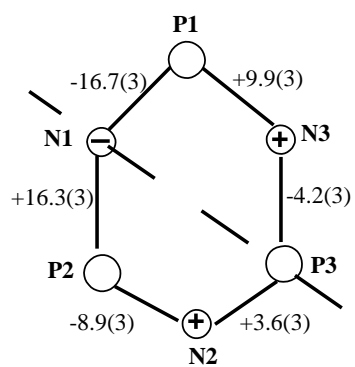
Figure S3. The conformations of the five-membered spiro-ring of **5**.



Figure S4. The conformations of the five-membered spiro-ring of **14**.



compound 5



compound 14

Figure S5. The shape of the phosphazene rings in **5** and **14** with torsion angles (deg).

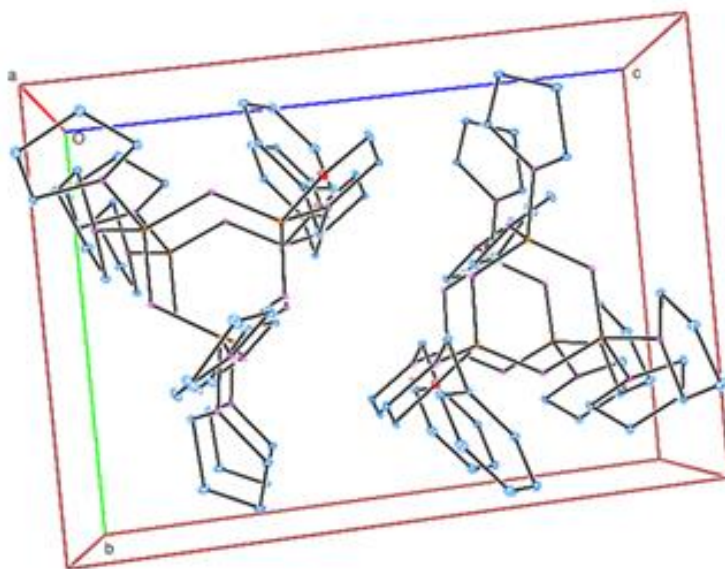


Figure S6. The packing diagram of **5**.

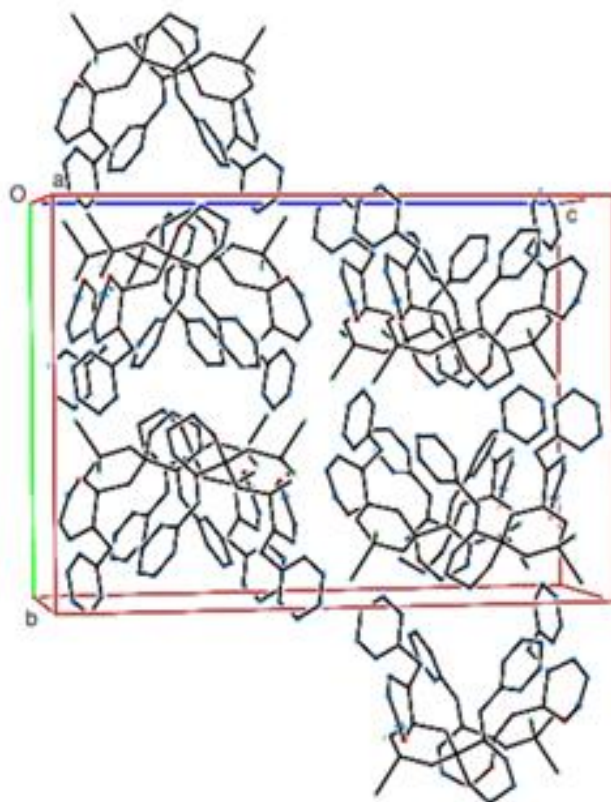


Figure S7. The packing diagram of **14**.